



Experimental study on slip flow of nitrogen through microchannels at atmospheric pressure

Yudong Zhang¹ · Shuaiwei Dou¹ · Junxia Qi¹ · Xianzhong Xu¹ · Jingjiang Qiu¹ · Zon-Han Wei^{1,2}

Received: 30 June 2022 / Accepted: 13 December 2022 / Published online: 28 December 2022
© The Author(s), under exclusive licence to Springer-Verlag GmbH Germany, part of Springer Nature 2022

Abstract

Gas flows through microchannels are commonly involved in various micro-electro-mechanical systems devices. Unlike the conventional flows at the macroscopic scale, micro-scale gas flows often show significant slip characteristics. This study designed a gas micro-flow measurement system based on the double-tank constant volume method to investigate the flow behaviors of gases through microchannels. The measurement system has a minimum mass flow rate resolution of 10^{-11} kg/s, which can meet the requirements of micro–nano-scale gas flow monitoring. We then investigated the slip flow characteristics of nitrogen in the microchannels at atmospheric pressure. The experimental data agreed well with the theoretical results based on the slip flow theory, which confirmed the existence of velocity slip in microchannels. In addition, we extracted the tangential momentum accommodation coefficients (TMAC) from the measured mass flow rates for different experimental conditions. The results showed that, in our experiment, the TMAC value ranged from 0.84 to 0.96 and tended to decrease with decreasing microchannel size.

1 Introduction

In recent years, with the rapid development of micro–nano-fabrication technology, a wide variety of micro-electro-mechanical systems (MEMS) devices have been developed. In many MEMS devices, such as micro-motors, accelerometers, micro-pumps, gas sensors, and lab-on-a-chip systems, flows of gases at the micro-scale are involved (Hak 2001; Fennimore et al. 2003; Yih et al. 2005; Okamoto et al. 2019; Yang and Dai 2015; Tao et al. 2020). Therefore, it is essential to investigate the characteristics and mechanisms of micro-scale flow (Gao et al. 2020; Yamaguchi et al. 2016; Agrawal 2011; Karniadakis et al. 2005), which can further guide the design and optimization of microdevices.

Unlike conventional macroscopic flow, gas flow exhibits strong non-equilibrium or discontinuity properties at the micro–nano-scale, such as velocity slip, temperature jump,

thermal creep flow, molecular transport, etc. (Wang et al. 2017; Ou and Chen 2020; Yamaguchi and Kikugawa 2021). The primary reasons are twofold. First, at the micro-scale, the characteristic size of the channel is close to the mean free path (MFP) of gas molecules, so the continuum model is no longer applicable. Second, the surface area-to-volume ratio in microdevices is significant; thus, surface-related factors, such as the wall slip effects, play a more substantial role in influencing the overall flow characteristics at the micro-scale¹⁴.

Previous studies on micro-scale gas flow mainly focus on theoretical calculations where the interaction at gas–solid interfaces is usually described using a diffuse reflection boundary model. However, the experiment results show that the complete diffuse reflection cannot accurately describe the slip flow characteristics of gases, so the Maxwell-type model (or Maxwell scattering model) with a combination of diffuse and specular reflections was proposed (Maxwell 1879). A tangential momentum accommodation coefficient (TMAC) is introduced in the Maxwell-type model to characterize the proportion of gas molecules that undergo diffuse reflection after collision with a wall (Maxwell 1879; Zhang et al. 2017). As a crucial interfacial parameter, the TMAC can describe the degree of velocity slip of fluid on a solid surface and is essential for accurately calculating mass flow in the slip

✉ Yudong Zhang
ydzhang@zzu.edu.cn

✉ Zon-Han Wei
profwei@zzu.edu.cn

¹ School of Mechanics and Safety Engineering, Zhengzhou University, Zhengzhou 450001, China

² Institute of Intelligent Sensing, Zhengzhou University, Zhengzhou 450001, China

flow regime. The value of TMAC depends on many factors, including gas species, surface materials, gas pressure, surface roughness, and surface temperature (Cao et al. 2009).

Generally, it is still challenging to obtain the TMAC directly from theoretical calculations. Since the TMAC is a function of mass flow rate, it can be calculated from the measured mass flow rate through a channel. For instance, Arkilic et al. (2001) introduced a dual-tank constant-volume method to measure the mass flow rate of helium through the channels under different pressure ratios. They fabricated microchannels with the same surface structure on silicon wafers and experimentally observed that TMACs are in the range between 0.75 and 0.85. Colin et al. (2004) also measured the mass flow rate across silicon microchannels using helium and nitrogen as working fluids. The experimental data are close to the slip model when TMAC is taken as 0.93. Yamaguchi et al. (2011) studied the characteristics of argon, nitrogen, and oxygen flow through deactivated-fused silica. They found that the TMAC is mainly determined by gas and surface material type. Silva et al. (2018) proposed a time-dependent constant volume method to measure the mass flow of nitrogen in microchannels accurately. They obtained that the TMAC value is 0.986 ± 0.019 in a stainless steel microtube. Perrier et al. (2019) measured the mass flow rate of gases in rectangular microchannels under isothermal conditions. In their study, the microchannels with different aspect ratios, surface materials, and roughness were experimentally investigated, and the velocity slip and TMAC values were calculated based on the Maxwell-type model.

In most works of literature, gas slip flow properties are investigated under vacuum conditions where the gas is highly rarefied. However, a majority of MEMS devices operate at atmospheric pressure, so it is necessary to study the flow characteristics of micro-scale gas flow under non-vacuum conditions. Moreover, at the micro-scale, the mass flow rate of gas is usually in the range between 10^{-8} and 10^{-13} kg/s. It is a great challenge to directly measure the mass flow rate in microchannels using a conventional commercial flowmeter. In this work, based on the constant-volume method, we first built a gas micro-flow measurement system capable of accurately measuring mass flow rates at the 10^{-11} kg/s orders of magnitude. Afterward, the mass flow rates of nitrogen through microchannels under various pressures close to the atmospheric pressure were measured and investigated using this system. Unlike the silicon or stainless steel surface used in previous experiments, the polydimethylsiloxane (PDMS) substrates were prepared with optical lithography and molding processes. Then, the microchannels were fabricated by bonding PDMS substrates with microchannel structures to a glass substrate. Experimental results were compared with theoretical calculations and numerical simulations to verify the accuracy of experimental measurements. Finally,

the TMAC value of nitrogen in various microchannels were measured and investigated.

The remainder of this paper is organized as follows. Section 2 introduces experimental method including the fabrication of microchannels, the experimental apparatus, the measurement technique, and device calibration. The results and discussion are given in Sect. 3 where the mass flow rates of nitrogen are calculated, the experimental data are compared with theoretical solutions, and the TMAC for various sizes of microchannels are investigated. The conclusion is given in Sect. 4.

2 Experimental apparatus and principle

2.1 Fabrication of microchannels

The schematic depiction of the microchannel used in the experiment is shown in Fig. 1. Five identical channels with rectangular cross section in micron size are arranged in parallel. This multi-channel structure can significantly reduce the errors associated with individual flow channel measurements by averaging the total mass flow rate. On the other hand, it is also possible to improve the detection accuracy by increasing the gas flow through the microchannel.

Figure 2 shows a schematic view of the microchannel fabrication process, including making the mask, fabricating microfluidic master mold in SU-8 negative photoresist, pouring PDMS mixture, and bonding to a glass substrate.

A detailed depiction of the mask fabrication sequence is given in Fig. 2a. First, a glass substrate was first deposited with a thin layer of Cr film (100 nm) as the hard mask for the etching (High Vacuum Evaporation System, ULVAC, ei-5z) and then covered by the positive photoresist AZ1500 4.4cp using a spin coater (Spin Soater, KW-4T). Next, the pattern on the mask was designed with Ledit software and exposed on the photoresist through a Table-Top Maskless Aligner (Heidelberg instruments, μ PG 101). Then, the photomask with the required microchannel pattern was

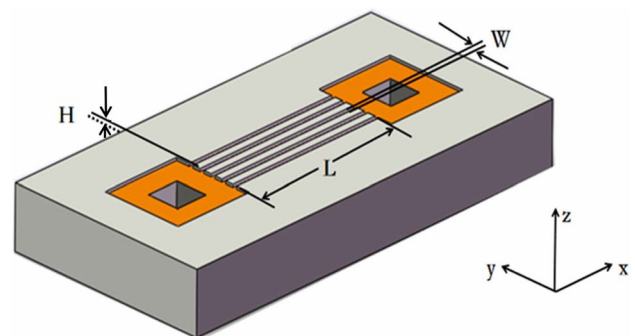


Fig. 1 Schematic of the microchannel

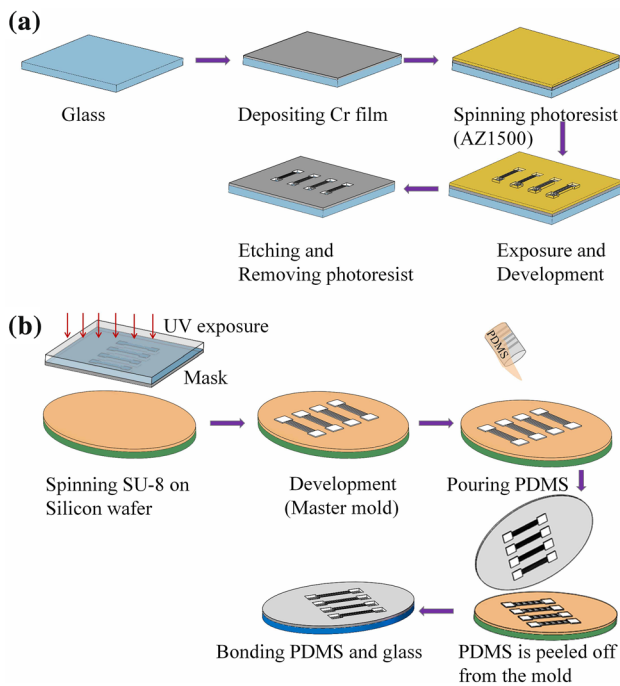


Fig. 2 Flow diagram of microchannel fabrication: **a** mask template and **b** PDMS microchannel

prepared through the processes of development, etching, and removal of excess photoresist. Finally, the resulting structure was measured with an optical microscope for critical size and defect inspection.

The schematic depiction of the PDMS microchannel fabrication sequence is shown in Fig. 2b; it mainly includes fabricating master mold, pouring PDMS mixture, and bounding to a substrate. The negative photoresist (SU-8 3005) was first spin-coated onto a 4-in. silicon wafer, and the mask was applied on an aligner for ultraviolet exposure. Then, the unexposed photoresist was removed through treatment with developer solution, and a master mold with the microchannel pattern was completed. The PDMS prepolymer and curing agent (Dow Corning, SYLGARD 184) were mixed in a ratio of 10:1 and removed excess bubbles, and then the PDMS mixture was poured on the master mold and cured at 75 °C for 2 h in a drying oven (ZHICHENG, ZXR-D-A7230). After that, the PDMS cured film was peeled off from the mold to obtain the PDMS substrate with a microchannel pattern. Then, a hole punch with a diameter of 0.5 mm was used to punch through holes at the inlet and outlet of the channel for subsequent experiments. Finally, the PDMS substrate was bounded to a glass substrate through oxygen plasma treatment with a plasma cleaner (CIF, CPC-B). Before further measurements, the connectivity of the microchannel is checked by injecting a colored liquid into the channel and then withdrawing it.

2.2 Experimental apparatus and measurement technique

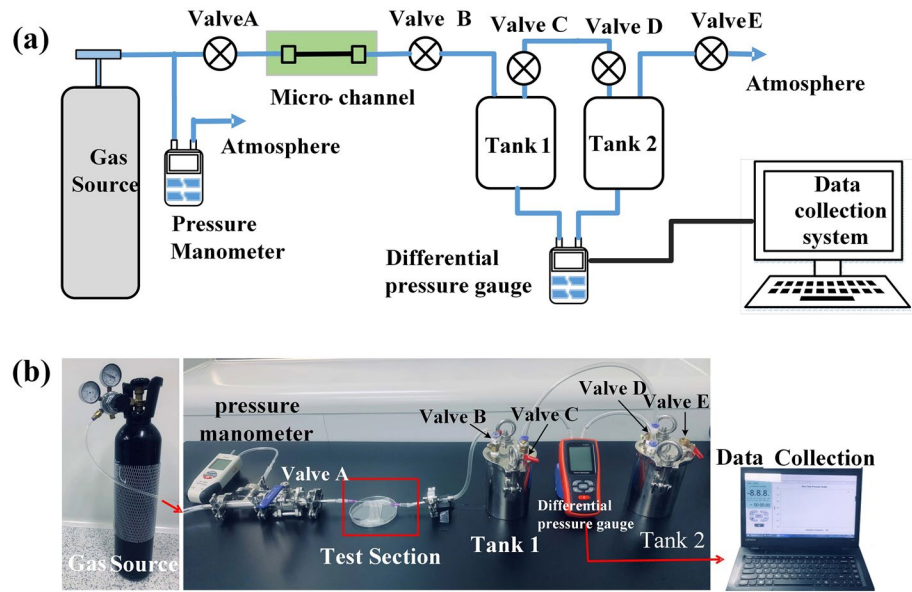
To measure the gas mass flow rate through microchannels, an indirect measuring method, i.e., constant-volume method is used. According to the gas equation of state, when a tank keeps the volume constant, the pressure variation inside the tank has a specific relationship with the variation of gas density; therefore, it is possible to get the flow rate of the gas by monitoring the pressure change of the tank. In this experiment, a double-tank constant-volume method is used to reduce the perturbation of tank pressure due to temperature fluctuations in the environment. The relative pressure difference between the two tanks was measured instead of the absolute pressure change of one tank. The two tanks were placed in the same environment. One of the tanks was used as a reference tank, so the perturbation caused by the ambient temperature can be maximally offset, thus achieving an accurate measurement of the mass flow rate.

The micro-gas flow experimental system is shown in Fig. 3. The schematic diagram of the experimental setup is shown in Fig. 3a to make it easier to understand, and photographs of the experimental apparatus is shown Fig. 3b. It consists of a high-pressure gas cylinder, a pressure regulator, a digital differential pressure manometer (SANLIANG, DP390), a microchannel test section, two gas storage tanks, a data collection system, some valves, and connection components. The parts of the experimental apparatus are connected through the standard vacuum connectors (KF-16) and PU pipes. The pressure manometer available for differential pressure measurements between two tanks has a typical accuracy of $\pm 0.25\%$ FSO (Full Scale Output), where the FSO is 2490 Pa. The connection or isolation of the two tanks can be achieved by switching valves on the tanks. The ambient temperature was measured with a thermocouple. Before the experiment, we conducted gas tightness tests on pipes and joints by soaking the entire connected pipe in water and simultaneously injecting gas from one end. We confirmed that the gas tightness was good, because there were no bubbles on the pipes or at the connectors.

Based on the experimental apparatus presented above, the micro-gas flow tests were conducted as follows:

- **Step 1:** Put the experimental apparatus in a stable temperature environment, open valves A, B, C, D, and E, and wait 10 min to ensure that the system was in equilibrium.
- **Step 2:** Open the high-pressure gas cylinder and adjust the pressure regulator to get the desired value in the inlet of the microchannel. Then, close the valve C, D, and E. The gas in the high-pressure gas cylinder flows through the horizontally placed experimental test section and finally into tank 1, causing changes in the reading of the pressure manometer between the two tanks.

Fig. 3 Micro-gas flow experimental apparatus: **a** schematic diagram and **b** actual photos



- **Step 3:** The differential pressure over time was stored in the computer through the data collection system, and the mass flow rate of gas flowing through the micro-channel was calculated from the differential pressure data.
- **Step 4:** Adjust the pressure of the high-pressure gas cylinder for the next set of experiments and repeat the above steps. The measurements were repeated several times for each condition.

The gas in the tank satisfies the ideal gas law, that is

$$pV = mR_m T, \tag{1}$$

where p and T are the pressure and temperature of the gas, V is the volume of the container, m denotes the mass of the gas, and R_m is the specific gas constant.

When the gas mass in the tank changes, the pressure, and temperature will also change because the volume of the tank is constant. For the double-tank constant-volume system, the mass flow rate can be written as follows:

$$\dot{m}_1 = \frac{V_1}{R_m T_1} \frac{dp_1}{dt} - \frac{V_2}{R_m T_2} \frac{dp_2}{dt} + \frac{p_2 V_2}{R_m T_2^2} \frac{dT_2}{dt} - \frac{p_1 V_1}{R_m T_1^2} \frac{dT_1}{dt}, \tag{2}$$

where the subscript “1” and “2” refer to the gas parameters within tank 1 and tank 2, respectively. The two tanks have the same volume, and tank 2 is used as a reference in this system.

It should be noted that the isothermal level is slightly lower because the two tanks are not in the same block of material, but it does not make a big difference in the measurement result. During the experimental measurement, two

tanks were placed in the same environment to ensure that they have the same temperature, i.e., $T_1 = T_2$, and experienced the same temperature fluctuations, i.e., $\frac{dT_2}{dt} = \frac{dT_1}{dt}$. Hence, the mass flow rate can be simplified as

$$\dot{m}_1 = \frac{V_1}{R_m T_1} \frac{d\Delta p}{dt} - \frac{\Delta p V_1}{R_m T_1^2} \frac{dT_1}{dt}, \tag{3}$$

where $\Delta p = p_1 - p_2$. In this experiment, $\Delta p/p \ll 1$ and $\Delta p V_1 / (R_m T_1^2) = \Delta p / (p m T_1)$, so the measurement error caused by temperature fluctuations can significantly reduced using the double-tank constant volume system. Furthermore, the temperature fluctuations of environment are minimal during the experiment process, so we can ignore the second term in Eq. (3) in the actual calculation, and then the mass flow rate can be rewritten in a simple form as

$$\dot{m}_1 = \frac{V_1}{R_m T_1} \frac{d\Delta p}{dt}. \tag{4}$$

During the tests, the V_1 , R_m , and T_1 remain constant, so the only physical quantity that needs to be measured is the change of pressure difference (Δp) over time.

2.3 Calibration of the experimental apparatus

To calculate the mass flow rate using Eq. (4), it is necessary to calibrate the volume of tank 1, V_1 . To achieve this goal, we pushed a certain volume of gas into the system at a specific rate using a syringe pump (Longer Pump, TJ-1A) instead of the high-pressure gas cylinder. Then, the slope between the volume of injected gas and the pressure change in tank 1 was obtained by linear fitting. The volume of tank 1 was calculated from the slope, which turned out to be 550 ml. The

value of V_1 then can be used to calculate the mass flow rate from the pressure change rate in subsequent measurements. A comparison of the measured mass flow rate calculated using Eq. (4) and the injection rate is shown in Fig. 4. Three repeated measurements were taken for each data point, and error bars were given in the figure. The solid line is the injection rate of the syringe pump and symbols are the measured data. The two sets of data agree well, which verifies that the calculated mass flow rate is accurate. The calibrated parameter would be used in the following measurements of mass flow rate through microchannels.

3 Results and discussion

3.1 Mass flow rate measurement

We obtained channels with characteristic scales at the micron level based on the microchannel fabricating process described previously, and measured the mass flow rate of the gas flowing through the microchannels on the experimental platform presented in the previous section. Nitrogen is used as the experimental gas. The height, width, and length of the microchannel read $H = 5.32 \mu\text{m}$, $W = 81.6 \mu\text{m}$, and $L = 7500 \mu\text{m}$, respectively. The pressure at the outlet of the channel remains constant at atmospheric pressure, and the ratio of input pressure to exit pressure varied in the range of 1.25 ~ 1.45. It should be noted that, during the experiments, the pressure at the microchannel outlet (P_o) cannot remain absolutely constant, because the gas continues flowing into the container connected to the outlet of the microchannel. However, the relative change in the P_o is minimal, no more than 0.2%, so the pressure ratio between the inlet and outlet and the

Knudsen number at the outlet can be regarded as constant during the measurement process. The values of some physical parameters of nitrogen and experimental conditions are listed in Table 1.

The most critical step to get the mass flow of gases in microchannels is to measure the change rate of pressure difference with time. During the experiment, the pressure difference value was measured using a digital differential pressure manometer and recorded by the data collection system. The variation of pressure difference with time satisfies a linear relationship, and the slope was obtained by linear fitting. The changes of differential pressure with time for a microchannel under various pressure ratios are shown in Fig. 5. When the pressure ratio are set as 1.25, 1.30, 1.35, 1.40, and 1.45, the corresponding slopes of pressure difference are 0.21788, 0.25850, 0.30980, 0.36444, and 0.44056, respectively. Then, the average mass flow rates can be solved using Eq. (4), and the values for a single channel are $2.69816 \times 10^{-10} \text{ kg/s}$, $3.20118 \times 10^{-10} \text{ kg/s}$, $3.83646 \times 10^{-10} \text{ kg/s}$, $4.51311 \times 10^{-10} \text{ kg/s}$, and $5.45575 \times 10^{-10} \text{ kg/s}$, respectively. From these data, we can see that the mass flow rates of the gas in the microchannel are in the order of magnitude of 10^{-10} kg/s , which is far above the measurement accuracy.

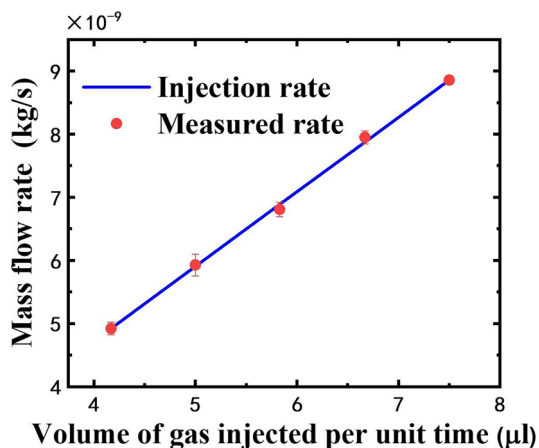


Fig. 4 Calibration chart for gas mass flow rate, where the solid line and symbols denote the injection rate of a syringe pump and the measured results using Eq. (5), respectively

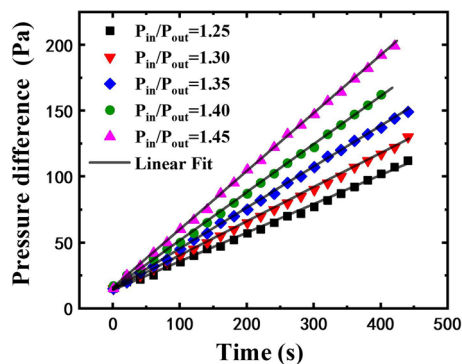


Fig. 5 Measured pressure differences with time

Table 1 Physical parameters of nitrogen and experimental conditions

Parameters	Values or Range
Gas constant (R)	8.314 J/(mol · K)
Viscosity coefficient (μ)	$1.77 \times 10^{-5} \text{ N}\cdot\text{s/m}^2$
Molar mass (M)	28 g/mol
Molecular MPF (λ)	$7.391 \times 10^{-8} \text{ m}$
Ambient temperature (T)	299.15 K
Outlet pressure (p_o)	101 KPa
Pressure ratio (p_r)	1.25 ~ 1.45

3.2 Slip flow theory and experimental data analysis

A no-slip model is commonly used in macroscopic flows, which assumes no relative motion between the fluid and the solid wall. However, this model is no longer reasonable, and the slip flow effect becomes significant when the Knudsen number (Kn) is large. The Kn is defined as the ratio of MFP of gas molecules to the characteristic scale, i.e., $Kn = \lambda/H$, and used to characterize the degree of discontinuity of a flow system. Navier first discussed solid–fluid interaction (Navier 1823), and then Maxwell introduced the concept of velocity slip (Maxwell 1879), pointing out that there may be a tangential velocity difference between the fluid and the solid surface which account for the non-continuum effects. Later, based on the two-dimensional Navier–Stokes equations and the Maxwellian slip boundary condition, Arkilic et al. (2001) derived the theoretical model for slip flow in microchannels. When taking the slip velocity into consideration, the mass flow rate in a microchannel can be expressed as

$$\dot{m} = \frac{H^3 W p_o^2}{24 \mu L R_m T} (P_r^2 - 1 + 12 \sigma K_o (P_r - 1)), \tag{5}$$

where H , W , and L are height, width, and length of the channel, respectively. μ denotes the viscosity coefficient of the gas, and P_r is the ratio of inlet pressure to outlet pressure, i.e., $P_r = p_i/p_o$. $\sigma = (2 - \alpha)/\alpha$ denotes the streamwise momentum accommodation, and α is the TMAC. K_o is the Knudsen number at the outlet of a microchannel.

To compare the experimental data with the no-slip theory, we plotted the ratio of the measured mass flow rate to the Poiseuille theory, \dot{m}/\dot{m}_p , in Fig. 6. \dot{m}_p denotes the theoretical results of Poiseuille flow, and its expression can be derived by dropping the last term in the parentheses in

Eq. (5). Theoretically, the slip effect decreases with the decrease of Knudsen number and tends to the non-slip case when the Kn goes to zero. There are two ways to reduce the Kn, which is to lower the MFP of gas molecules or increase the microchannel size. Since our experiment is carried out under atmospheric pressure, the MFP of gas molecules is almost constant. Thus, a feasible way to reduce the Kn is to increase the size of the microchannel. On the other hand, our experimental setup can only measure tiny amounts of gas, and it may be easily out of the range of measurement if the size of the channel is too large. Nevertheless, we can check the trend of the measured data approaching the theoretical results of the Poiseuille flow. As shown in Fig. 6, the value of \dot{m}/\dot{m}_p decrease with the reduction of Kn. We further compared the experimental data with the theoretical values in a wider range of Knudsen numbers in the inset, where the theoretical values are given by $1 + 6Kn$. It can be seen that the experimental data are well distributed on the curve of the theoretical solution, and the result approaches one as the Kn keeps going down.

The experimentally measured mass flow rates under different pressure ratios are shown in Fig. 7. The analytical solutions are also plotted for comparison. The analytical solutions were solved using Eq. (5) and the TMAC in slip theory is taken as 0.90. The no-slip analytical solutions can be obtained by setting $K_o = 0$. It can be seen that the mass flow rates given by the no-slip theory significantly deviate from the experimentally measured values. In contrast, the results of the slip theory are in good agreement with the experimental data, which indicates that there is a significant velocity slip in the gas flow in the microchannel.

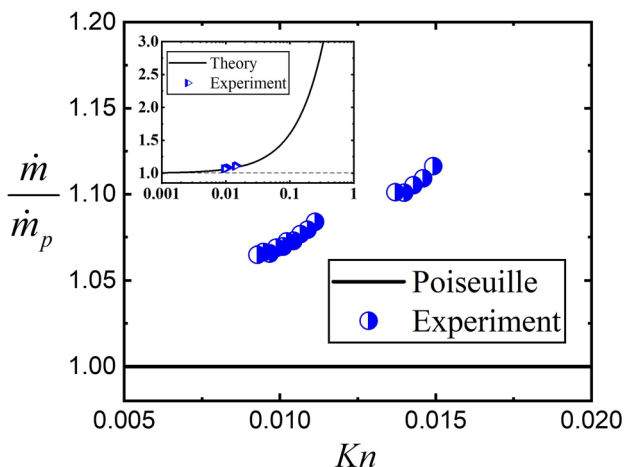


Fig. 6 Comparison between experimental mass flow rates and the results of non-slip theory

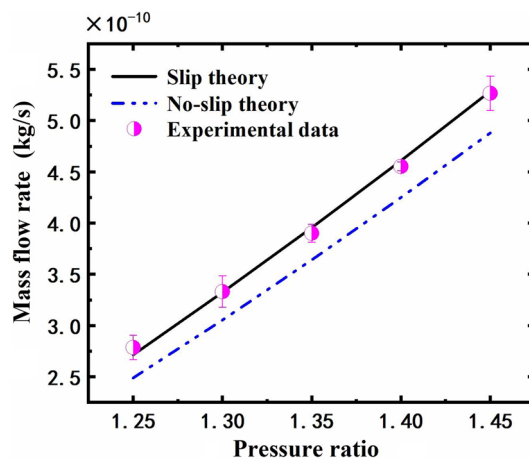


Fig. 7 Nitrogen mass flow rates at different pressure ratio

3.3 Determination of TMAC for different microchannels

The TMAC is an important parameter when describing the gas slip flow at the micro-scale. The degree of velocity slip on the solid surface can be characterized by the value of TMAC, representing the average tangential momentum exchange between the flowing gas molecules and the solid surface. The value of the TMAC is defined as

$$\alpha = \frac{\tau_i - \tau_r}{\tau_i - \tau_w}, \tag{6}$$

where τ_i is the average incident tangential momentum of gas molecules, τ_r is the average reflected tangential molecules, and τ_w is the tangential momentum of the solid surface. $\tau_w = 0$ when the solid surface is fixed. If gas molecules are diffusely reflected after colliding with the wall, then $\tau_r = 0$, which corresponds to $\alpha = 1$. Conversely, if gas molecules are specularly reflected after colliding with the wall, then $\tau_r = \tau_i$, which corresponds to $\alpha = 0$. When one part of the gas molecules is specular reflected and another part is diffusely reflected, $0 < \alpha < 1$.

The study of TMAC can help understand the transport laws at the gas–solid surface and reveal the physical nature of interfacial phenomena. In addition, it can also provide suitable parameters for the use of boundary models. Over the past few decades, researchers have measured this parameter through a series of experiments (Karniadakis et al. 2002; Maurer et al. 2003; Ewart et al. 2007; Graur et al. 2009; Yamaguchi et al. 2012). Available literature indicates that TMAC values typically range from 0.2 to 1.0, with the lower limit being for exceptionally smooth surfaces, and TMAC values are close to 1 for many actual surfaces. Experimental results also show that the TMAC is usually around 0.9 for theoretical analysis and numerical calculations when monatomic gases flow in common surface materials (for instance, silicon, glass, stainless steel, etc.). In contrast, for polyatomic gases, the value of TMAC has not been entirely determined. On the other hand, the TMAC values in the literature are mostly measured under certain vacuum conditions. Although rarefied gas and micro-scale flow have similarities, they may not be completely equivalent.

To investigate the variation characteristics of TMAC at atmospheric pressure, we use PDMS mixtures as surface materials to experimentally measure the mass flow rate of nitrogen in various microchannels and calculate value of TMAC based on Eq. (5). Three microchannels with different characteristic sizes used in the experiments are listed in Table 2. Measurement uncertainties are also listed in the table.

Based on this experimental apparatus in Fig. 3 and the calculation method of Eq. (4), we obtained the mass flow

Table 2 Geometric sizes of three different microchannels

Microchannel number	Height (μm)	Width (μm)	Length (μm)
Channel 1	4.4	78.5	7500
Channel 2	5.9	76.0	7500
Channel 3	6.5	80.0	7500
Uncertainty	±0.05	±0.5	±1

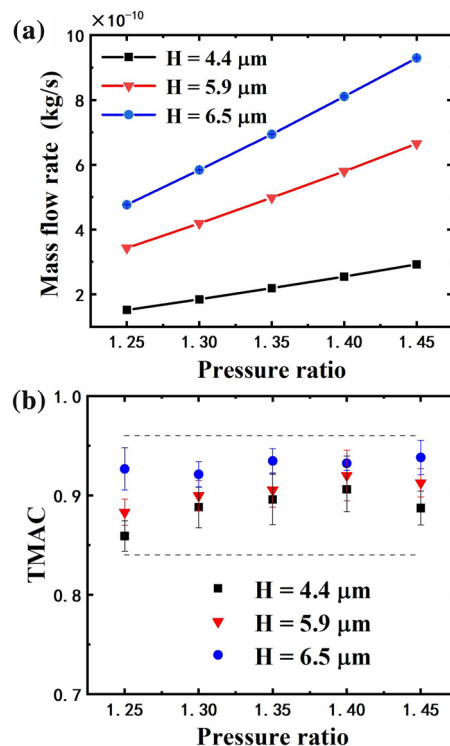


Fig. 8 Measurement results of nitrogen flow through different microchannels: **a** mass flow rate and **b** TMAC values. The error bars in the mass flow rate are not perceptible, because the error is small, on the order of 10⁻¹² kg/s

rates of nitrogen for three different microchannels. The measured mass flow rates as a function of the pressure ratio between inlet and outlet are shown in Fig. 8a. Each measurement was repeated three times, and the error bars are given in the figure, but they are not perceptible, because the error is very small, on the order of 10⁻¹² kg/s. All variables in Eq. (5) are known or measurable except for TMAC, so the value of TMAC can be calculated by the following formula:

$$\alpha = K_o / \left[\dot{m} \frac{\mu L R T}{H^3 W p_o^2} \frac{1}{(P_r - 1)} - \frac{(P_r + 1)}{24} + \frac{1}{2} \right]. \tag{7}$$

The TMAC values calculated from the measured mass flow rates in Fig. 8a are shown in Fig. 8b. It can be seen that the TMAC is not a constant value for microchannels with

different characteristic scales, and the values of TMAC for nitrogen flowing in these microchannels under atmospheric conditions range from 0.84 to 0.96. In a certain range, there is a tendency for TMAC to increase with the increase of the pressure ratio, but the influence of the pressure ratio on TMAC is not monotonous. With the microchannel characteristic size decrease, the TMAC has an evident tendency to decrease.

Experiments on gas flow at the nano-scale show that the gas flow exhibits super slip properties (Keerthi et al. 2018); the TMAC is close to 0 and the reflection of the gas molecules from the wall is almost completely specular. Although our experiment was conducted at the micro-scale, the experimental measurements are consistent with the findings of that work. The surface of PDMS cannot be atomically smooth, so the value of TMAC is not small as Ref. Keerthi et al. (2018). In fact, an atomically flat surface does not necessarily lead to a small TMAC. For example, the mass flow rate of gas through the atomically flat molybdenum disulfide (MoS_2) channel can be well prescribed by the Knudsen theory (diffuse reflection boundary), while the mass flow rate through the graphene or hBN channel is two orders of magnitude larger. Different from previous works, our experiment is measured under atmospheric pressure, and the gas flow regime is classified as slip flow rather than free molecular flow. The characteristics of TMAC of gas slip flow under atmospheric pressure are rarely reported. Here, based on our experimental results, a reasonable possibility is proposed that the TMAC may decrease with the reduction in scale.

There are many possible factors to affect the TMAC, such as the wall materials, surface morphology, surface roughness, gas species, etc. We measured the surface roughness of the microchannel by the atomic force microscope. The surface topography maps of the microchannel wall are shown in Fig. 9. The measurement results show that the amplitude of the surface fluctuation is less than 1.5 nm and the root-mean-square roughness (Rq) is about 0.43 nm which is much smaller than the height of the channel. On the other hand, the relative roughness should generally increase the TMAC value by increasing the chance of diffuse reflection after the molecules collide with the wall (Sun and Li 2008; Zhang et al. 2012). However, our experimental results show that the larger the relative roughness (corresponding to the smaller channel height), the smaller the TMAC value. Therefore, it is unlikely to be due to surface roughness.

It is generally believed that the gas flow at the micro/nano-scale is similar to the flow of macroscopic rarefied gas, since both kinds of flow have a large Knudsen number. However, we suspect that micro/nano-scale gas flow may have some unique properties, because the wall effect should be more significant at the micro/nano-scale. From the measured data, we found that, at atmospheric pressure, the decrease in the characteristic size of the system causes an increase in

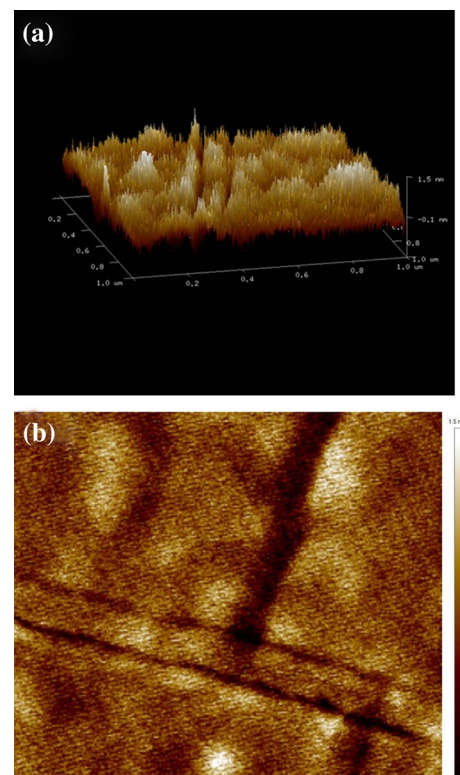


Fig. 9 Surface roughness characteristics of microchannel wall measured by atomic force microscopy: **a** three-dimensional topography map; **b** two-dimensional contour map. The area range in the figure is $1 \mu\text{m} \times 1 \mu\text{m}$. The amplitude of the surface fluctuation is less than 1.5 nm, and the measured root-mean-square roughness (Rq) is about 0.43 nm

the TMAC, which is potentially a difference between micro/nano-scale gas flow and macroscopic rarefied gas flow. It should be noted that this may not be a general conclusion, because more different types of wall and gas species are yet to be tested in the future. Nevertheless, our results are consistent with some previous findings in the literature. For example, it shows that the value of TMAC decreases with the increase of the Knudsen number for diatomic gases in Ref. Agrawal and Prabhu (2008).

3.4 Analysis of measurement uncertainty

Before the measurement, we first ensured that the experimental device had good gas tightness as introduced in Sect. 2.2, so the measurement error caused by the gas leakage can be ignored. The differential pressure gauge has a precision of $\pm 0.25\%$ FSO, where the FSO is 2490 Pa. Hence the uncertainty of the pressure difference $\delta(\Delta P)$ is approximately ± 6.25 Pa.

Generally, we measured the pressure change induced by five identical microchannels arranged in parallel for about

10 min to calculate the change rate of pressure; thus, the uncertainty of pressure change rate reads

$$\delta\left(\frac{\Delta P}{dt}\right) = \frac{\pm 6.25}{5 \times 600} = \pm 2.08 \times 10^{-3} \text{ Pa/s.} \quad (8)$$

According to Eq. (4), the uncertainty of mass flow rate is

$$\delta\dot{m} = \frac{V_1}{R_m T_1} \delta\left(\frac{\Delta P}{dt}\right) = \pm 1.29 \times 10^{-11} \text{ kg/s.} \quad (9)$$

This shows that the measurements of gas mass flow rates can be accurate up to 10^{-11} kg/s.

When it comes to the value of TMAC, according to the expression of Eq. (7), the relative error can be calculated as

$$\frac{\delta\alpha}{\alpha} = \frac{\delta G}{G}, \quad (10)$$

where $G = \dot{m} \frac{\mu L R T}{H^3 W p_0^2 (P_r - 1)} - \frac{(P_r + 1)}{24} + \frac{1}{2}$. According to the operation of uncertainty

$$\delta G = G_1 \left(\frac{\delta\dot{m}}{\dot{m}} + \frac{\delta L}{L} + 3 \frac{\delta H}{H} + \frac{\delta W}{W} \right), \quad (11)$$

where $G_1 = \dot{m} \frac{\mu L R T}{H^3 W p_0^2 (P_r - 1)}$, and δL , δH , and δW are uncertainty of length, height, and width of microchannel, respectively, whose values are given in Table 2. Thus the uncertainty of TMAC can be rewritten as

$$\frac{\delta\alpha}{\alpha} = \frac{G_1}{G} \left(\frac{\delta\dot{m}}{\dot{m}} + \frac{\delta L}{L} + 3 \frac{\delta H}{H} + \frac{\delta W}{W} \right), \quad (12)$$

If we take the smallest channel which has the maximum uncertainty as an example, the value of $\delta\alpha/\alpha$ is approximately ± 0.0139 . Take α as 0.9, and then $\delta\alpha$ is approximately ± 0.0125 .

From the above analysis, it can be seen that the uncertainty of the measured TMAC is about 1.25%, which is much less than the difference between the values of TMAC of different microchannels size, especially for the difference between microchannels with $H = 4.4 \mu\text{m}$ and $H = 6.5 \mu\text{m}$.

4 Conclusions

A double-tank constant-volume system was designed to measure the gas flow characteristics through microchannels. This design can significantly reduce the measurement errors caused by ambient temperature fluctuations. The experimental system has a resolution of 10^{-11} kg/s, so it can detect tiny amounts of gas mass flow rate without expensive commercial flowmeters. Based on this system, we measured the mass flow rate of nitrogen through the microchannels at atmospheric pressure and compared the experimental data with the theoretical solution of Navier–Stokes equations

combined with Maxwellian slip boundary condition. The experimental data agree well with the slip theory, which verifies the slip effect in the microchannel and the accuracy of the measurement method in this paper. Moreover, we obtained the TMAC values of nitrogen in different microchannels based on the slip flow model and the experimentally measured mass flow data. It was found that under the gas and microchannel conditions used in this experiment, there was a tendency for TMAC to decrease with decreasing the characteristic size of the microchannel.

Acknowledgements This work was supported by the National Natural Science Foundation of China under Grant No. 12102397 and the China Postdoctoral Science Foundation Grant No. 2019M662521.

Declarations

Conflict of interest The authors declare that they have no conflict of interest.

Data availability The data that support the findings of this study are available from the corresponding author upon reasonable request.

References

- Agrawal A (2011) A comprehensive review on gas flow in microchannels. *Int J Micro-Nano Scale Transp* 2:1–40
- Agrawal A, Prabhu SV (2008) Survey on measurement of tangential momentum accommodation coefficient. *J Vacuum Sci Technol A Vacuum Surf Films* 26:634–645
- Arkilic EB, Breuer KS, Schmidt MA (2001) Mass flow and tangential momentum accommodation in silicon micromachined channels. *J Fluid Mech* 437:29–43
- Cao B, Sun J, Chen M, Guo Z (2009) Molecular momentum transport at fluid–solid interfaces in MemS/Nems: a review. *Int J Mol Sci* 10:4638–4706
- Colin S, Lalonde P, Caen R (2004) Validation of a second-order slip flow model in rectangular microchannels. *Heat Transf Eng* 25:23–30
- Ewart T, Perrier P, Graur I, Meolans JG (2007) Tangential momentum accommodation in microtube. *Microfluid Nanofluid* 3:689–695
- Fennimore AM, Yuzvinsky TD, Han WQ, Fuhrer MS, Cumings J, Zettl A (2003) Rotational actuators based on carbon nanotubes. *Nature* 424:408–10
- Gao R, O’Byrne S, Sharipov F, Liow JL (2020) Experimental investigation of the separation of binary gaseous mixtures flowing through a capillary tube. *Phys Fluids* 32:112008
- Graur IA, Perrier P, Ghozlani W, Meolans JG (2009) Measurements of tangential momentum accommodation coefficient for various gases in plane microchannel. *Phys Fluids* 21:102004
- Guo Z, Li Z (2003) Size effect on single-phase channel flow and heat transfer at microscale. *Int J Heat Fluid Flow* 24:284–298
- Hak M (2001) Flow physics in MEMS. *Mec Ind* 2:313–341
- Karniadakis GEM, Beskok A, Gad-El-Hak M (2002) Micro flows: fundamentals and simulation. *Appl Mech Rev* 55:B76
- Karniadakis G, Beskok A, Aluru NR (2005) Microflows and nanoflows: fundamentals and simulation. Springer, Berlin
- Keerthi A, Geim AK, Janardanan A, Rooney AP, Esfandiari A, Hu S, Dar SA, Grigorieva IV, Haigh SJ, Wang FC (2018) Ballistic molecular transport through two-dimensional channels. *Nature* 558:420–424

- Maurer J, Tabeling P, Joseph P, Willaime H (2003) Second-order slip laws in microchannels for helium and nitrogen. *Phys Fluids* 15:2613–2621
- Maxwell JC (1879) On stresses in rarified gases arising from inequalities of temperature. *Philos Trans R Soc Lond* 170:231–256
- Navier C (1823) Memoire sur les lois mouvement des fluides. *Mem l'Acad R Sci de l'Inst France* 6:389–440
- Okamoto Y, Ryoson H, Fujimoto K, Ohba T, Mita Y (2019) On-chip cmos-mems-based electroosmotic flow micropump integrated with high-voltage generator. *J Microelectromech Syst* 29:86–94
- Ou J, Chen J (2020) Nonlinear transport of rarefied Couette flows from low speed to high speed. *Phys Fluids* 32:112021
- Perrier P, Hadj-Nacer M, Meolans JG, Graur I (2019) Measurements and modeling of the gas flow in a microchannel: influence of aspect ratios, surface nature, and roughnesses. *Microfluid Nanofluid* 23:1–22
- Silva E, Deschamps CJ, Rojas-Ciárdenas M, Barrot-Lattes C, Baldas L, Colin S (2018) A time-dependent method for the measurement of mass flow rate of gases in microchannels. *Int J Heat Mass Transf* 120:422–434
- Sun J, Li Z (2008) Effect of gas adsorption on momentum accommodation coefficients in microgas flows using molecular dynamic simulations. *Mol Phys* 106:2325–2332
- Tao Z, Sun J, Li H, Huang Y, Wu H (2020) A radial-flux permanent magnet micromotor with 3d solenoid iron-core mems in-chip coils of high aspect ratio. *IEEE Electron Dev Lett* 41:1090–1093
- Wang S, Lukyanov AA, Wang L, Wu YS, Pomerantz A, Xu W, Kleinberg R (2017) A non-empirical gas slippage model for low to moderate Knudsen numbers. *Phys Fluids* 29:012004
- Yamaguchi J, Kikugawa G (2021) Molecular dynamics study on flow structure inside a thermal transpiration flow field. *Phys Fluids* 33:012005
- Yamaguchi H, Hanawa T, Yamamoto O, Matsuda Y, Egami Y, Niimi T (2011) Experimental measurement on tangential momentum accommodation coefficient in a single microtube. *Microfluid Nanofluid* 11:57–64
- Yamaguchi H, Matsuda Y, Niimi T (2012) Tangential momentum accommodation coefficient measurements for various materials and gas species. *J Phys Conf* 362:012035
- Yamaguchi H, Takamori K, Perrier P, Graur I, Matsuda Y, Niimi T (2016) Viscous slip coefficients for binary gas mixtures measured from mass flow rates through a single microtube. *Phys Fluids* 28:657
- Yang MZ, Dai CL (2015) Ethanol microsensors with a readout circuit manufactured using the cmos-mems technique. *Sensors* 15:1623–1634
- Yih TC, Wei C, Hammad B (2005) Modeling and characterization of a nanoliter drug-delivery mems micropump with circular bossed membrane. *Nanomed Nanotechnol Biol Med* 1:164–175
- Zhang W, Meng G, Wei X (2012) A review on slip models for gas microflows. *Microfluid Nanofluid* 13:845–882
- Zhang Y, Xu A, Zhang G, Chen Z (2017) Discrete Boltzmann method with Maxwell-type boundary condition for slip flow. *Commun Theor Phys* 69:77–85

Publisher's Note Springer Nature remains neutral with regard to jurisdictional claims in published maps and institutional affiliations.

Springer Nature or its licensor (e.g. a society or other partner) holds exclusive rights to this article under a publishing agreement with the author(s) or other rightsholder(s); author self-archiving of the accepted manuscript version of this article is solely governed by the terms of such publishing agreement and applicable law.